Hydrodynamic behaviour of floating wind turbines

Difference between linear and non-linear wave effects on wave induced fatigue loads in a spar-type floating wind turbine

Master of Science Thesis – Short Public Version

Author:	**Jorrit Roy Bergsma**	
Committee:	Prof. dr. ir. R.H.M. Huijsmans	TU Delft Chairman
	Dr.ir. A. Romeijn	TU Delft
	Dr.ir. S.A. Miedema	TU Delft
	Dr.ir. P.L.C. van der Valk	Siemens
	Ir. H.M. Tilanus	Siemens

November 2015

Due to confidentiality restrictions some data is normalized or left out.
This data is included in the report. This report is not shared online.

TU Delft Delft University of Technology

SIEMENS

1 INTRODUCTION

1.1 Thesis objective and relevance

Huge developments in bottom founded turbines have been made since the start of offshore wind energy, mainly in Europe. In many countries outside of Europe, steep coasts permit no bottom-fixed foundations. The solution for this problem is floating wind turbines (FWT). Up to now, several concepts of FWTs have been designed and a couple of prototypes have been installed. Research on the different concepts of FWTs has advanced over the past ten years, and several aero-elastic tools have been developed. Non-linear wave effects have often been ignored in modelling the hydrodynamic behaviour of FWTs, under the assumption that they are significantly smaller than linear wave effects. In addition, only a few studies have been conducted on fatigue loads in floating wind turbines.

Therefore, the objective of this thesis is to assess the non-linear hydrodynamic effects on wave induced fatigue loads in a spar-type FWT. Non-linear hydrodynamic effects, or second-order wave effects, cause extra loads on the turbine at the sum and difference frequencies of the incident waves. The sum and difference frequencies cover a frequency range that can overlap with structural eigenfrequencies of the FWT, which could lead to resonant excitations that cause significant fatigue damage to the structure. Therefore, it is important to investigate how second order wave loads affect the fatigue response of a FWT. The analysis is focused on the fatigue loads at the tower bottom, since its design is fatigue driven. The main contributor for the fatigue at the tower bottom is the oscillations of the bending moment. The overall goal of this thesis is to answer the question whether and when second-order wave effects should be included in computer simulations of FWTs.

The main research question is formulated as:

> *What is the difference between the first order wave effects versus second order wave effects on the wave induced fatigue loads of a spar-type floating offshore wind turbine?*

1.2 Applied FWT concept

A catenary moored spar-type FWT inspired by the Hywind Demo concept is considered in this study. Hywind Demo, from Statoil, is world's first full scale spar-type FWT and is installed at the Norwegian coast. Hywind Demo is composed of three parts: a spar-buoy substructure, a tower and a Siemens 2.3 MW wind turbine generator. Based on Hywind Demo other designs called OC3-Hywind and Hywind Scotland have been developed. In Table 1.1 the main properties of Hywind Demo are presented.

Table 1.1 - Main properties of Hywind Demo

Item	Dimension
Turbine	Siemens 2.3-MW
Water depth (m)	200
Draft (m)	100
Hub height above MWL (m)	65
Displacement (m)	5036
Static centre of buoyancy (m) under MWL	-51,03
Diameter at MWL (m)	6,0
Diameter at bottom (m)	8,3
Mass total FWT (ton)	5086
Centre of gravity of total FWT (m)	-67,48
Mass moment of inertia I_{xx} and I_{yy} floater (ton*m²)	$29{,}24 \cdot 10^8$
Mass moment of inertia I_{zz} (ton*m²)	$9{,}17 \cdot 10^4$
Height of mooring connection (m)	-53,0

Figure 1.1 - Dimensions of Hywind Demo turbine

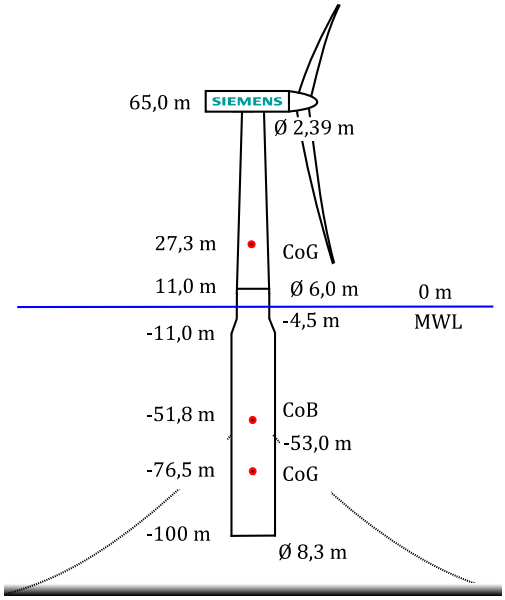

2 Model set-up

2.1 Multibody description

For studying the difference in fatigue loads due to linear and non-linear waves, a hydro-elastic model has been developed in Matlab. The model is a multibody description that captures the first structural eigenmode, the spar and tower are both represented by one rigid body. The first eigenmode is of particular interest, as it overlaps with the wave's non-linear sum-frequencies. The MBD method that is applied to derive the equations of motions at every time step is the TMT-method, which is proposed in the lecture notes 'Multibody Dynamics B' [5].

Figure 2.1 - Schematic overview of developed model

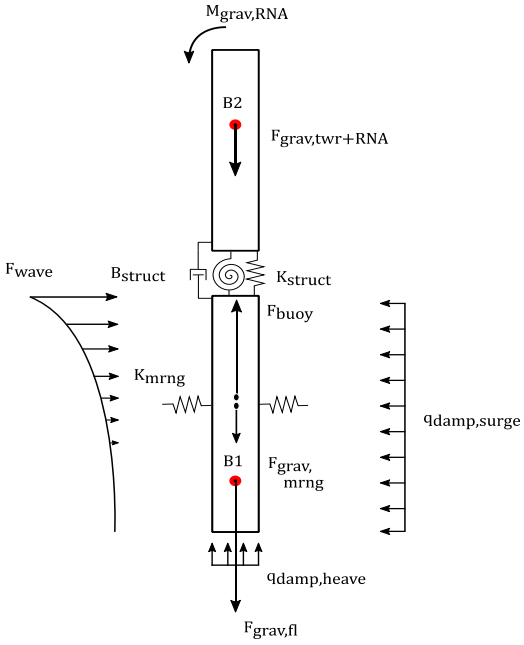

Accelerations of the floater in water induces forces that are related to added mass. The added mass terms are included via an extra mass term in the mass matrix in the EoM. This implies a linearization of the added mass its frequency-dependence, which is regarded as acceptable based on [1].

2.2 Structural stiffness and damping

The structural damping is accounted for as dashpots between the bodies of the MDOF-model. The damping of the dashpots is determined by taking a percentage of the critical damping, called *damping ratio.* The damping ratio of $\zeta = 1$ % is chosen based on [1], which is the value for welded steel in working stress level.

The structural stiffness is accounted for as springs between the bodies of the MDOF-model. The stiffness of the springs is determined using mechanics on the stiffness of cylinders. An enhanced explanation of the basic mechanics is to be found in [*4*]. The rotational stiffness, together with the rigid body masses, determines the structural eigenfrequency in bending. The tower bending eigenfrequency in the model is similar to eigenfrequency of the design.

2.3 Platform stiffness: hydrostatics and mooring

Hydrostatic stability is induced by the gravity and buoyancy force. The buoyancy force is calculated with the alternating submerged point, so it allows for pressure differences in vertical direction and thus includes the influence of waves on the heave motion. The hydrostatics provide restoring only for heave, roll and pitch. Restoring in the other modes of motion must be realized by the mooring system.

The influence of the mooring lines is modelled as linear springs that act in the horizontal plane and a static downwards force, which mimics the weight of the mooring cables. Linear springs are regarded as sufficient, since the displacement of the mooring-attachment point appeared to be <4 *m,* even for severe sea states. The horizontal displacement are smaller than expected, probably due to exclusion of (unidirectional) wind and current.

2.4 (Non-)linear wave kinematics

When modelling irregular waves with second order effects, the result is a non-linear random wave model. The recommended non-linear random wave model, according to DNV standards [6], is the second-order perturbation model by Longuett-Higgins [2]. The linear model, based on potential flow theory, is extended with second-order terms.

The first- and second-order irregular waves are generated using SWAG (Siemens Wave Generator). This tool is developed in-house by Siemens Wind Power and is used as a pre-process tool to set-up data of wave kinematics for different sea states. In SWAG a kinematic data field is computed that is loaded into the self-made model. SWAG is based on potential flow theory, and the linear model is extend with second-order perturbation model by Longuett-Higgins [2]. Fast Fourier transform (FFT) is used to generate the desired time history. The FFT method is applied, it is suitable due to its computational efficiency. For describing the wave kinematics up to current the free water line Wheeler stretching is used.

In SWAG the diffraction effects are accounted for via a MacCamy-Fuchs correction [3]. In the approach of MacCamy-Fuchs the correction includes a modification of the inertia coefficient C_M and a phase-lag on the inertia force. The diffraction correction mainly influences larger wave numbers, which are related to the sum-frequencies. The computed wave spectra are described by a JONSWAP-spectrum with a cut-off frequency at 4 times the peak frequency.

2.5 Wave forces

The self-made model cannot be coupled directly with SWAG, since SWAG calculates the wave kinematics in the frequency domain and cannot account for platform motions in horizontal direction. Therefore a small addition is made to the SWAG code, which results in the following implementation: the wave kinematics are pre-calculated for a 2D grid in which the floater will move. At every time step the position and orientation of the floater is known. Over the vertical of the floater there is a *fluid point* every meter, over which the hydrodynamic forces are calculated. The related kinematics in the wave field grid are extracted from the pre-processed kinematics file, and the kinematics at the fluid points along the spar are determined via interpolation. In vertical direction the wave kinematics grid points are more densely packed around MWL, since the water velocities and accelerations are greatest in this area. Also the differences in wave kinematics between linear and non-linear waves are biggest around MWL.

The Morison equation is used to calculate hydrodynamic forces on circular cylindrical structural members. The damping forces appear through the relative velocity. The basic Morison formula does not include heave excitation. The heave excitation is included via pressure integration in the heave direction.

2.6 Time integration method

The solution for the equation of motion is calculated for every time step, using a Matlab build in function ODE45. This is an ordinary differential equation (ODE) solver, which applies an explicit Runge-Kutta(4,5) formula. The accuracy of ODE solver greatly depends on the tolerance settings.

2.7 Fatigue loads

Within this study the sum of fatigue loads per simulation are compared between different cases. By applying rain flow counting of half-cycles on the load series the equivalent fatigue loads are determined. The advantage of this method is that all peaks are determined without doubling.

The total fatigue loads of a simulation are expressed as normalized equivalent fatigue load, applying Miner's rule. The number of cycles per amplitude bin are first normalized to the same simulation duration (1-hour), then the total fatigue loads per amplitude bin are summed up and finally the sum is divided by a number of reference cycles. The normalized equivalent fatigue load can be interpreted as the magnitude of the force cycle that, when it is applied 10^7 (N_{ref}) times, leads to the same amount of fatigue loading as the fatigue loading measured in the 1-hour equivalent of the simulation. From here on the normalized equivalent fatigue load will be shortly referred to as equivalent fatigue load, or EFL.

3 VERIFICATION

The self-made model is verified by comparing the results with results from the thoroughly verified model BHawC. The verified characteristics are static equilibrium, natural frequency and damping of the platform motions, natural frequency of tower bending and the response to waves in terms of motion and internal forces.

All these model characteristics seem to agree well with results from BHawC, with small differences in internal horizontal force, tower bending eigenfrequency and platform damping. These differences are below 10% and can be declared by the difference in implementation methods of both models. Therefore the differences between both models are regarded acceptable.

4 RESULTS

4.1 Overview of studies

Two studies have been conducted in this thesis. The first study contains a statistical analysis of the fatigue loads, for different simulation durations and different number of realizations per sea state. The second study focuses on the difference in fatigue loads caused by linear versus non-linear waves.

Chosen load cases

The applied sea states range calm sea states to severe states in five ascending steps (sea states no. 1-5 in Table 4.1). Also are two extra sea states applied with peak frequencies around half the tower bending eigenfrequency (sea states no. 6-7 in Table 4.1). In order to investigate the effect of second order waves around the eigenfrequency of the tower in more detail and to analyze the influence of significant wave height separately.

Different simulation durations are used, i.e. 10, 60 and 180 minutes. For all sea states linear and non-linear waves have been simulated for the three durations of simulation.

Table 4.1 - Sea states of load cases

Sea state	H_s [m]	T_p [s]	Characteristics
1	1,00	4,80	Smooth
2	1,40	6,50	Slight
3	2,44	8,10	Moderate
4	3,66	9,70	Rough
5	5,49	11,3	Severe
6	1,40	4,35	Slight
7	1,80	4,35	Moderate

4.2 Statistical analysis

Statistical dispersion for different simulation durations

The variance in EFL for different simulation times is analyzed. Figure 4.1 provides better insight in this variance. Here, the median and variance of sea state numbers 6 and 17 for different simulation times are presented. Due to computational problems the 180-min simulation results are solely included for sea state number 10. The presented data show a much smaller spacing of the quartiles in the boxplots for longer simulation times. This means that the seed dependent dispersion of the EFL decreases for increasing simulation time. The mean of the estimated fatigue loads appear independent of simulation duration.

Figure 4.1 – Median and variance of EFL for different sea states and simulation times. Resp. 20,20,10 seeds, for 10min,1hr,3hr.

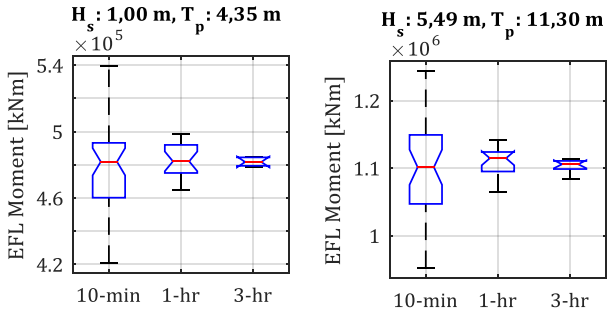

Figure 4.2 – Boxplots of EFL for different "snap-shots" in 60-min simulation. 20 seeds

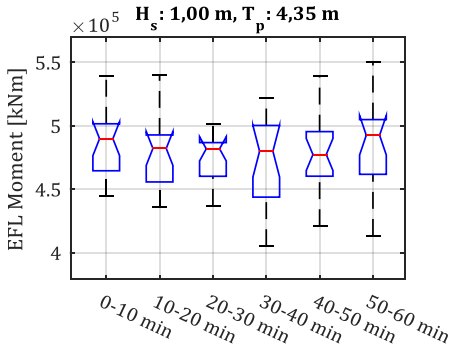

Fatigue load dependence on simulation time

Additionally, the assumption that longer simulation time relate to higher fatigue loads is investigated. This assumption is based on the possibility that low frequent platform motions need more time to be fully induced, than the used 10 min plus 200s build-up time. From Figure 4.2. the difference between the mean EFL of 10 minutes at different moments in time is negligible and varying. Therefore it is concluded that simulation time does not influence the estimation of the EFL $M_{y,towerbottom}$.

4.3 Fatigue analysis

The difference in fatigue loads caused by linear versus non-linear waves is analyzed. Regarding the wave kinematics of linear versus non-linear waves, there is an important difference between the energy

distributions over frequencies. In non-linear waves, energy is displaced from around peak frequency towards higher sum frequencies, which are around twice the peak frequency. Also energy is displace towards lower-difference frequencies, which are slightly above 0 *Hz*.

The results of 1-hour simulations of multiple sea states with increasing severity are compared. The power differences between linear versus non-linear waves are regarded in two ways. Firstly as the "absolute difference with respect to the highest energy peak in the linear spectrum", named *normalized absolute difference,* and defined as $PSD_{absDiff,norm} = (PSD_{NL} - PSD_L) / P_{L,peakFreq}$. Secondly, as the "relative difference between the linear and the non-linear simulation", named *relative difference*, and defined as $PSD_{relDiff} = (PSD_{NL} - PSD_L) / PSD_L$. In this paper only two sea states are presented due to space limitations. These results are chosen, since they are representative for other sea states as well.

Comparing fatigue loads for different sea states with linear and non-linear waves

In calm sea states, the fatigue loads at tower bottom are 5% to 20% higher for non-linear waves than for linear waves, as shown in Figure 4.3. The main reason is the extra energy in the excitation forces at frequencies around twice the peak frequency, related to the second-order sum frequencies, as shown in Figure 4.4. These frequencies overlap with the tower bending eigenfrequency and are strongly amplified in the response (see Figure 4.5)

In contrast to calm sea states, the rougher sea states cause 3% to 10% higher fatigue loads for linear waves comparing with non-linear waves (Figure 4.3). The linear waves contain more energy around the wave peak frequency and around the pitch eigenfrequency (see Figure 4.4). Significantly more energy is present around these frequencies in the bending moment response, leading to higher fatigue loads (see Figure 4.5).

Figure 4.3 – Difference in EFL of bending moment at tower bottom for multiple realizations of five different sea states

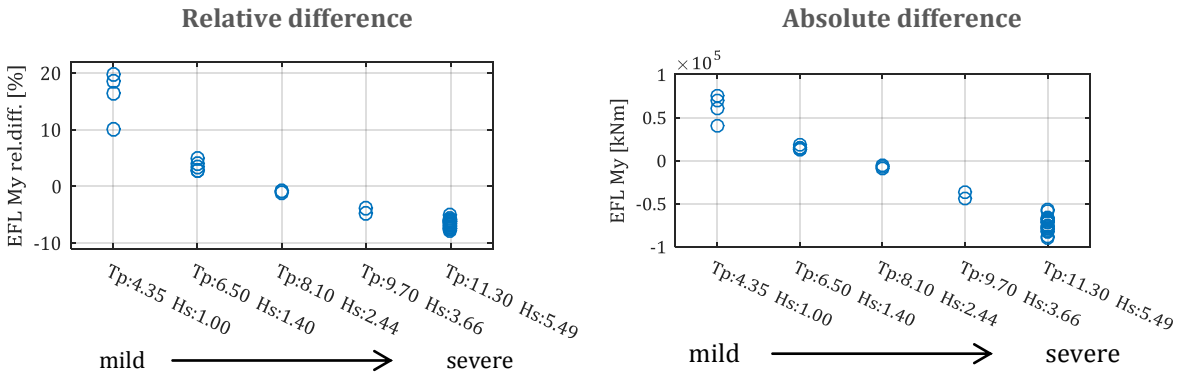

Figure 4.4- PSD of Wave Elevation - *normalized absolute difference (above) & relative difference (below)*

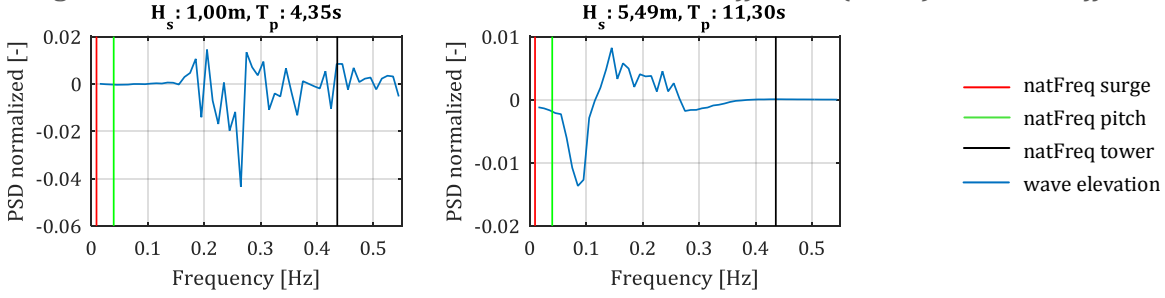

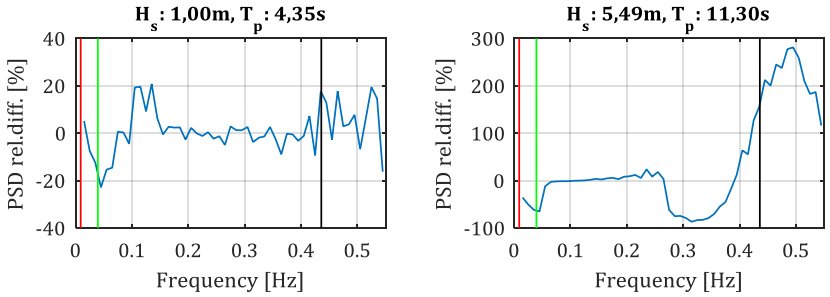

Figure 4.5- PSD of Tower Bending Moment - *normalized absolute difference (above) & relative difference (below)*

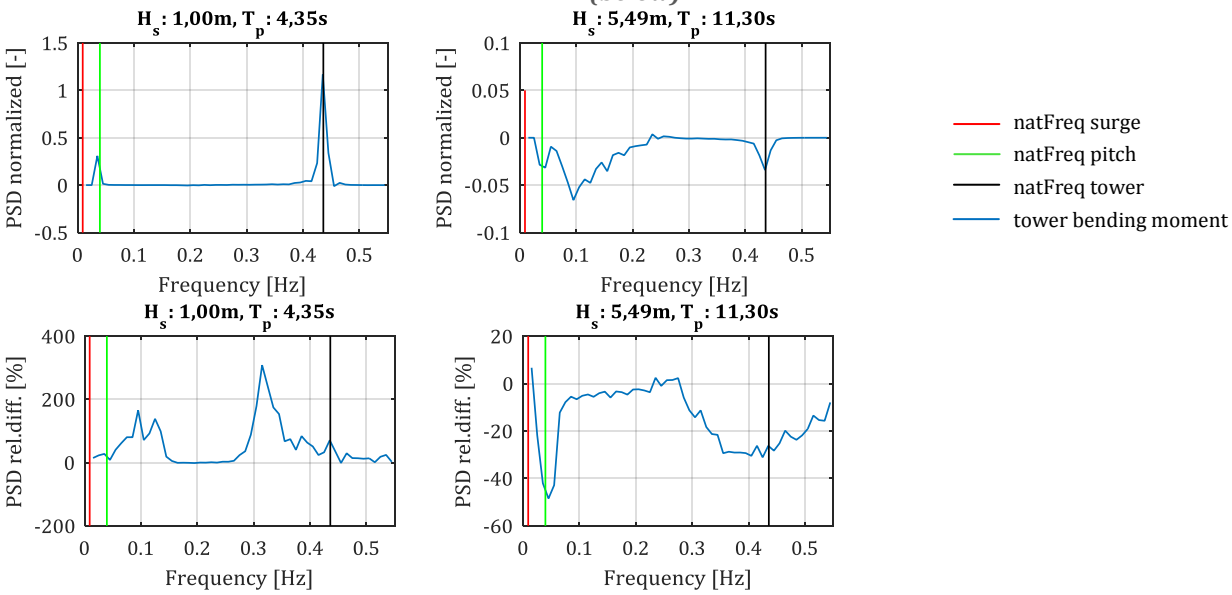

High amplification around eigenfrequency

Based on a frequency-amplification test is concluded that the bending moments at tower bottom could be highly amplified for excitation forces with a frequency around the tower bending eigenfrequency. The amplification is strongly dependent on the structural damping. Therefore the structural damping of the tower bending should be chosen with care. Furthermore significant amplification is present around the platform's pitch eigenfrequency and, to some extent, around the eigenfrequency of surge.

Dependence on significant wave height and peak period

Beside the previous cases, three additional sea states with different significant wave heights and same peak periods are compared. This comparison gives an impression of the influence of significant wave height on the difference in EFL (see Figure 4.6). For the three sea states, the EFL caused by non-linear waves is higher than it is for linear waves. One could expect that when having the same peak period: the higher the significant wave height, the more energy the spectrum contains, the higher the (absolute) difference in EFL will be. Neither the absolute difference, nor the relative difference in fatigue loads has a clear-cut relation with the significant wave height. Nonetheless, the three sea states have in common that non-linear waves lead to higher fatigue loads, giving the impression that this relates to the peak period.

When extrapolating the hypothesis that the difference in fatigue loads depends on the peak period, based on the available results, it gives reasons to assume that for sea states with a peak period below 6,5 *s,* and maybe even below 7,5 *s,* non-linear waves lead to higher fatigue loads than linear waves do.

However, to draw a strongly founded conclusion, more different combinations of significant wave heights and peak periods need to be determined.

Occurrence probability at existing location

Finally, based on scatter diagram data of a existing suitable location (not included in this paper for confidentiality reasons), it is concluded that the overall occurrence probability of sea states that lead to higher fatigue loads when non-linear effects are included, lies between 18% and 63%. For these sea states, the estimated fatigue loads are 5% to 20% higher for non-linear waves than for linear waves.

Figure 4.6 - EFL of bending moment at tower bottom for sea states with different H_s

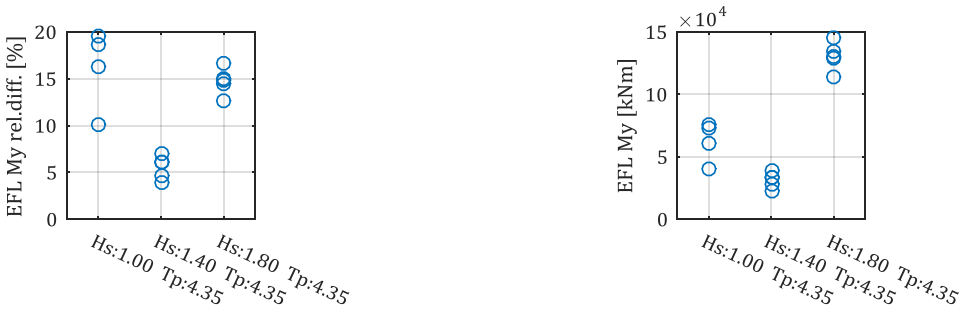

4.4 Conclusions

The design of the tower bottom of a spar-type floating wind turbine is fatigue driven. The main contributor for the fatigue are the oscillations in bending moment. The fatigue loads of the bending moment at tower bottom have been analyzed for different sea states and simulation lengths. Between different realizations of the same sea state significant variance of the fatigue loads is seen. A statistical analysis of different simulation times showed that the equivalent fatigue load (EFL) based on 10-min simulations varies 20% between different realizations. In 60-min and 180-min simulations the EFL varies 4% and 1% respectively.

While it is found that the variance between EFLs is higher for shorter simulation time, the mean of the EFLs appears to be independent of simulation time: the mean of the EFL is similar for 10-min, 60-min and 180-min simulations. Also, the difference between the mean EFL of 10-min snapshots at different moments in time during a longer simulation is negligible.

The statistical dispersion of the difference in EFL due to linear and non-linear waves is smaller for the 60-min simulation than the 10-min simulation. This coincides with the previous results. Therefore it is decided to use 60-min simulations for further analyses.

The EFLs due to linear and non-linear waves have been compared for multiple sea states of increasing severity. For the five analyzed mild sea states, with peak periods below 7,5 *s* and significant wave heights below 2 *m*, the fatigue loads at tower bottom are 5-20% higher for non-linear waves than for linear waves. This is mainly because extra energy is present around twice the peak frequency, due to the inclusion of second-order sum-frequencies. For these sea states the sum-frequencies overlap with the tower bending eigenfrequency. The power of excitation forces around tower bending eigenfrequency leads to a significant increase of bending moments, due to resonance amplification.

The sea state with peak period of 8,1 *s* and significant wave height of 2,44 *m*, has the same EFLs for linear and non-linear waves. For the more severe sea states, with peak periods above 9 *s* and significant wave heights above 2 *m*, linear waves lead to 3-10% higher fatigue loads than non-linear waves. The linear waves of these severe sea states contain more energy around the wave peak frequency and around the pitch eigenfrequency, resulting in more energy around these frequencies in the bending moment response and consequently leading to higher fatigue loads. For more severe sea states, with longer wave periods, the sum-frequencies do not have any significant overlap with the tower bending eigenfrequency. Hence resonance around these frequencies has negligible effect, in contrast to milder sea states.

The transfer-function of hydrodynamic forces to bending moments at tower bottom is found to have a high amplification for frequencies around the tower for-aft bending eigenfrequency. The way of incorporating the structural damping has strong influence on this amplification. Therefore the damping ratio of the structural damping should be chosen with care.

In addition three mild sea states with different significant wave height and same peak period have been compared, in order to examine the influence of significant wave height on the difference in fatigue loads. Neither the absolute difference, nor the relative difference in fatigue loads has a clear-cut relation with the significant wave height. Nonetheless, the three mild sea states have in common that non-linear waves lead to higher fatigue loads, which suggests a relation to the peak period. When this suggestion is extrapolated based on the available results, it gives reasons to assume that for sea states with a peak period below 6,5 *s* - and maybe even below 7,5 *s* - non-linear waves lead to higher fatigue loads than linear waves. However, more different combinations of significant wave height and peak period need to be compared to draw a well founded conclusion.

Finally it is considered what the occurrence probability of the effects would be at an existing location where the Hywind Demo turbine could be installed. The overall occurrence probability of sea states that lead to higher fatigue loads when non-linear effects are included is between 18% to 63%, depending on range of sea states that is assumed to correspond with this effect. Concerning the sea states in which linear waves lead to higher fatigue loads it is hard to draw a conclusion, since too few results are available for waves with peak periods above 8 seconds.

4.5 Recommendations

In this study the difference in fatigue loads due to linear and non-linear waves are analyzed by comparing sea states with increasing severity. Also, three sea states with similar peak period and increasing significant wave height are analyzed. In order to substantiate conclusions about the influence of the parameters significant wave height and peak period on the difference in fatigue loads, a parametric study needs to be executed where as many realistic combinations of these parameters as possible are compared. Beside this, the influence of the design of the should be analyzed, because this could have a major influence on the response and the resultant fatigue loads.

In order to couple the frequency-domain tool SWAG with the self-made time-domain model, a method is applied which led to a model with high memory use and long computation times. Another disadvantage of the applied method is that insight in the difference between linear and non-linear waves can solely be

obtained via the differences in time series of the computed kinematics and structural response of a separate linear and non-linear simulation. This method is applied due to the limited development time-frame of this study, which did not allow for suitable alternatives to the applied method. For following studies, it is advised to integrate a time-domain wave kinematics tool. This could drastically improve the computation time and makes it possible to analyze the contributions of linear and non-linear effects separately.

Since wind forces are excluded in this study, it is not possible to draw conclusions about the influence of non-linear wave effects on the fatigue loads in relation to the wind induced fatigue loads. Also controller effects and the effect of aerodynamic damping are not incorporated. The amplification around the tower bending for-aft eigenfrequency is high, especially for lower damping ratios. Aerodynamic damping could have a significant influence on decreasing resonance effects in tower bending, mainly in case of unidirectionality between wind and waves. Consequently, aerodynamic damping could have a large influence on decreasing the bending moments and related fatigue loads. When excluding the aerodynamic damping, the calculated bending moments are likely to be overestimated.

Due to the discretization in the fast Fourier transformation, a part of the results is non-smooth. In this study 5-20 simulations are applied, providing useful but non-smooth results. In order to get smooth results it is recommended to run a minimum of 40 simulations per sea state. Smart windowing in the FFT could also lead to smoother results.

5 REFERENCES

[1] Jason Mark Jonkman. *Definition of the Floating System for Phase IV of OC3*. National Renewable Energy Laboratory Golden, CO, USA, 2010.

[2] Michael S Longuet-Higgins and RW Stewart. Radiation stresses in water waves; a physical discussion, with applications. In *Deep Sea Research and Oceanographic Abstracts*, volume 11, pages 529–562. Elsevier, 1964.

[3] RC MacCamy and RA Fuchs. Wave forces on piles: a diffraction theory. Technical report, DTIC Document, 1954.

[4] David-P Molenaar and Sjoerd Dijkstra. Modeling the structural dynamics of flexible wind turbines. In *EWEC-CONFERENCE-*, pages 234–237, 1999.

[5] Richard Q. van der Linde and Arend L. Schwab. Multibody dynamics b - lecture notes. Lecture Notes TU Delft, 1997.

[6] Det Norske Veritas. Dnv-rp-c205 environmental conditions and environmental loads. *Norw ay: DetNorskeVeritas*, 2010.